

Nonlinear response analysis for T-shaped structures having new acoustic black hole with residual thickness supported by nonlinear springs

Takao Yamaguchi^{1, a,*}, Chihiro Kamio^{1, b}, Shinichi Maruyama^{1, c},
Tomohiro Tanaka^{2, d} and Ryoichi Fujinuma^{2, e}

¹Gunma University, 1-5-1 Tenjin-cho, Kiryu, Gunma, 376-8515 Japan

²Graduate School of Gunma University, 1-5-1 Tenjin-cho, Kiryu, Gunma, 376-8515 Japan

*Corresponding author

^a<yamagme3@gunma-u.ac.jp>, ^b<chihiro.kamio@gunma-u.ac.jp>,

^c<maruyama@gunma-u.ac.jp >

Keywords: acoustic black hole, nonlinear spring, finite element method, damping, nonlinear response

Abstract. This paper reports numerical analysis using FEM with Model Strain Energy Method for structures having a T-shaped cross section supported by nonlinear concentrated springs under impact load. An edge of the rib plate in the T-shaped structure has an Acoustic Black Hole with residual thickness. A viscoelastic damping layer is covered on the black hole. Finite element for the nonlinear springs with hysteresis are expressed and are connected to the T-shaped structures modeled by linear solid finite elements in consideration of complex modulus of elasticity. We calculated modal loss factors and transient responses using eigenmodes including coupled motions between the nonlinear springs and the T-shaped structures. From the dominant modes and the impact responses, we clarified effects of the black hole with residual thickness on the nonlinear damped responses. By adding the black hole to the structures, modal loss factors increase. Higher modal loss factors are obtained due to set the residual thickness. As the amplitude of the impact force increases, the responses become complicated due to the nonlinearity, and include more super harmonic and subharmonic components. The nonlinear components are reduced by adding the black hole. The less nonlinear components are given due to set the residual thickness.

1. Introduction

Recently, some researchers have been studying acoustic black holes as an effective approach of vibration damping or vibration reduction. A concept was proposed by Mironov [1] to realize small amplitudes in structures using an acoustic black hole in case of the resonance. Mironov studied propagations of bending waves in a flat plate having an edge where the thickness of the plates is decreasing to the edge as a quadratic function x^2 of the distance x from the boundary. Due to this structure, the bending waves cannot reflect at the edge. However, to obtain vibration reduction effects using Mironov's acoustic black hole, it is required that the length of the edge is enough long. At the edge, extraordinary thin thickness is necessary. This results in the acoustic black hole is ideal and cannot be applied in practical use. To improve this problem, Krylov modified the Mironov's acoustic black hole [2]-[5]. He cut off the edge practically as finite length. He also added a thin viscoelastic damping layer on the top of the edge. This Krylov's acoustic black hole has high damping with light weight. On the other hand, Oberst [6] theoretically analyzed vibration damping effects of a straight metal beam covered with a viscoelastic layer. He revealed that the effects of the damping layer are proportional to (thickness of the damping layer/ thickness of the metal beam)². The thickness of the edge in the black hole is extraordinary thin. If a viscoelastic damping layer is laminated on the edge in the black hole, high efficient damping effects appear. The length of the edge in the black hole can be

shortened with keeping the vibration reduction. To obtain damping effects in the lower frequency region, Tang proposed “Residual thickness” [7]. The residual thickness means that the edge is extended as minimum thickness keeps after the thickness decreases according to the power function for the acoustic black hole. Nevertheless, these structures having the acoustic black holes have local regions including extraordinary thin thickness. Thus, when we try to add these acoustic black holes to actual structures in practical use, it contains difficulties due to the weakness of thin thickness for strength of the structure, as shown in Fig.1(a). To solve this problem, we proposed that around the edges of beads or ribs in panels, height of the bead or rib decreases according to the power functions for the acoustic black hole, as shown in Fig.1(b) [8]. This enable us that it is not necessary to use the extraordinary thin thickness in the local regions of the panels with the acoustic black holes.

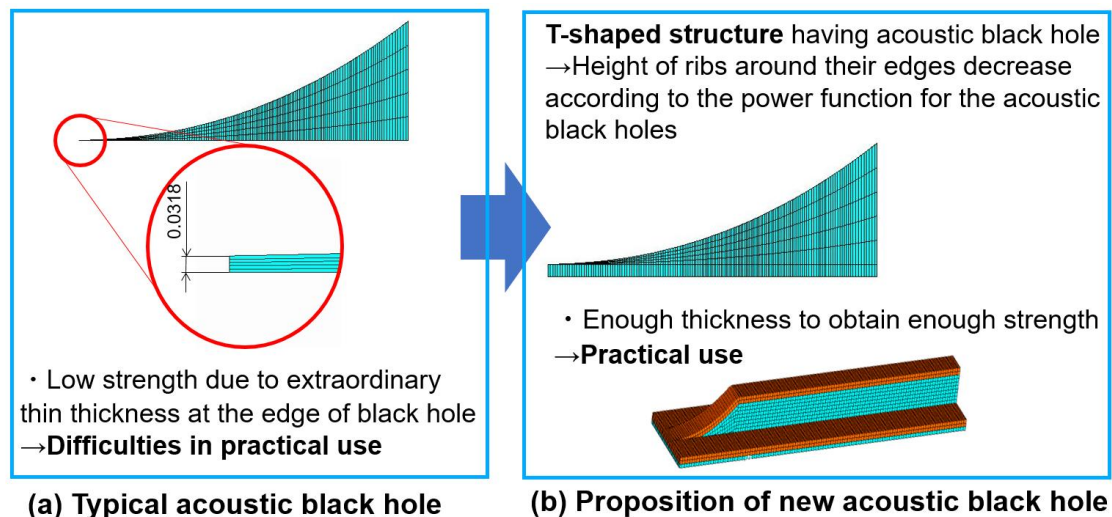


Fig.1. Problems in strength at the edges around acoustic black holes and proposition of new acoustic black hole.

On the other hand, vibration isolation using concentrated springs have been used to protect lightweight structures from undesirable impacts. But, these lightweight structures sometimes do not have high rigidity. For these cases, the structures should be regarded as elastic bodies. When the structures for isolation are constituted of polymer materials, these structures are necessary to consider as viscoelastic bodies. Further, some concentrated springs have nonlinear relations between displacement and load. Thus, we have been studying dynamics for the coupled problem between elastic bodies and viscoelastic bodies and nonlinear springs using finite element method including normal coordinates corresponding to linear natural modes.

Many researchers have been studying the nonlinear vibration problems for systems including concentrated mass and concentrated spring. Freeny investigated Proper Orthogonal Modes for this system [9]. Shaw proposed Nonlinear Modal Analysis and applied to a simply supported beam attached to a nonlinear concentrated spring at midpoint of the beam [10]. Yamaguchi et. al. [11-13] previously proposed a fast computation method to obtain the nonlinear vibrations in an elastic block or a viscoelastic block or a sound-proof structure supported by a nonlinear concentrated spring with linear hysteresis.

Nevertheless, dynamics for structures having acoustic black holes with viscoelastic layers connected with nonlinear springs have not been clarified yet.

To evaluate effects of the acoustic black holes on reduction of nonlinear vibration, this paper deals with vibration analysis using finite element method for T-shaped structures having acoustic black holes connected with nonlinear concentrated spring under impact loads. The structure includes a T-shaped cross section. Around the edge of the rib plate in the T-shaped structures, the height of the rib decreases

according to the function for the Krylov’s acoustic black hole. We also examine effects of addition of the residual thickness. A viscoelastic damping layer is covered on the regions around the black hole. The restoring force of the nonlinear springs is assumed to be expressed as power series of displacement. The restoring force has linear hysteresis damping. Therefore, complex stiffness is introduced for the linear component of the restoring force. Finite elements for the nonlinear springs are expressed and are connected to the T-shaped structures having the acoustic black holes with viscoelastic layers modeled by linear solid finite elements. The discrete equations in physical coordinate are transformed into the nonlinear ordinary coupled equations using normal coordinate corresponding to linear natural modes [11-13]. In this process, modal damping is also transformed using Modal Strain Energy Method. The transformed equations in the normal coordinates are integrated numerically in small degree-of freedom.

We calculate modal loss factors and transient responses using eigenmodes including coupled motions between the nonlinear springs and the T-shaped structures having the acoustic black holes. From the dominant modes and the time histories, we clarify effects of the acoustic black hole with / without residual thickness on the nonlinear damped responses.

2. Calculation Models

To examine effects of the acoustic black holes on reduction of nonlinear vibration, we use three calculation models as shown in Figs. 2, 3 and 4. Figure 2 shows FEM model for a T-shaped structure having flanges and a rib. Then, this structure includes a T-shaped cross section. The height of the rib is 50 [mm]. Thickness of the two flanges are 5.04 mm.

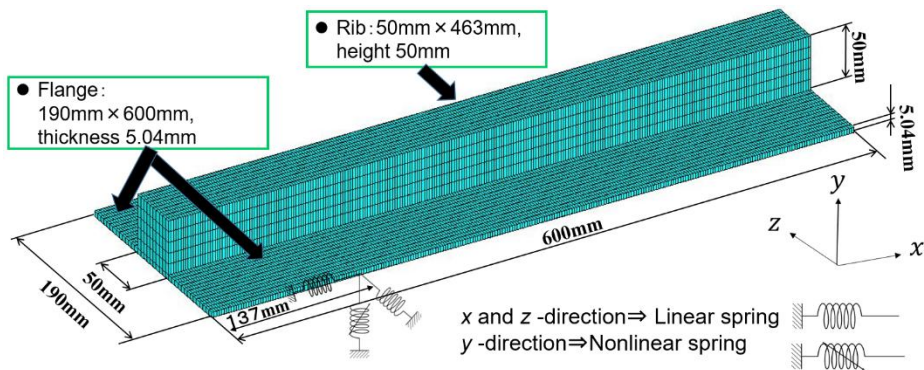


Fig. 2. FEM model for T-shaped structure without acoustic black hole and viscoelastic layer.

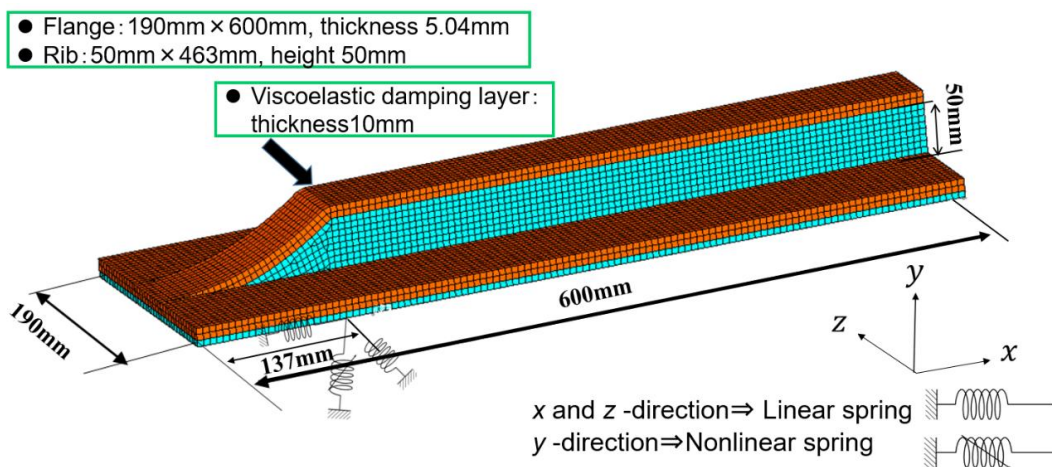


Fig. 3. FEM model for T-shaped structure having acoustic black hole with viscoelastic layer.

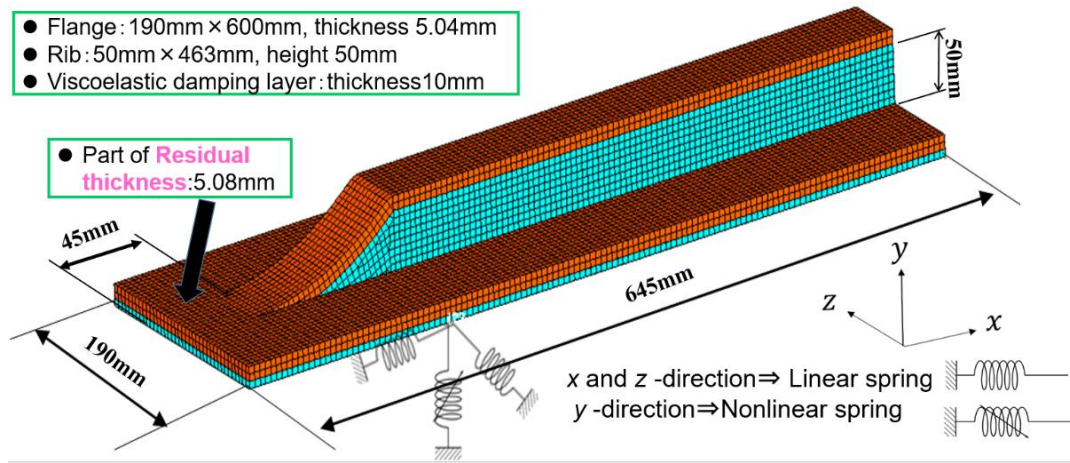


Fig. 4. FEM model for T-shaped structure having acoustic black hole with viscoelastic layer (Including residual thickness).

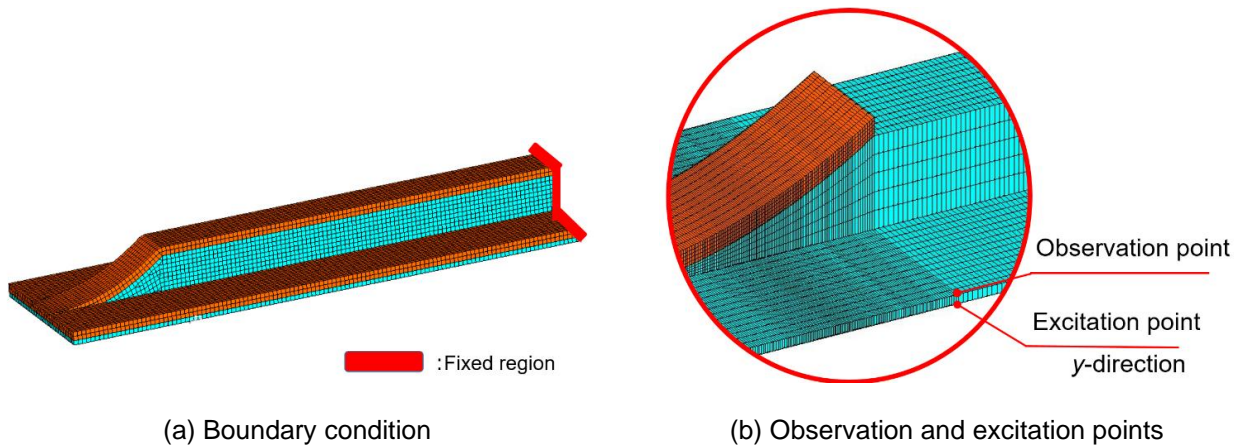


Fig.5 Boundary condition and observation point and excitation point

This structure is connected with two nonlinear concentrated springs in y -direction as can be seen in Fig.2. And in x - and z - directions, linear springs are attached at the same points. Here, note that the nonlinear and linear springs are attached to the symmetrical position in Fig.2 about the x -axis. An impact loads are exerted to get nonlinear responses. As shown in Fig.3, we give the new acoustic black holes at one edge of the rib in the T-shaped structures. Around the edge of the rib plate, the height $h(x)$ of the rib decreases according to the function $h(x) = \varepsilon x^{2.2}$ for the Krylov's acoustic black hole. Where, x is the distance from the edge. A viscoelastic damping layer is covered on the regions around the black hole and on the flanges. Thickness of the damping layer is 10 [mm]. We added residual thickness to the new T-shaped structure having the acoustic black hole in Fig.4. The length of the region having residual thickness is 45 [mm]. One end of these T-shaped structures are fixed as shown in Fig. 5(a). The excitation point and observation point are illustrated in Fig. 5(b).

3. Calculation Procedure

3.1. Discretized Equation for Nonlinear Concentrated Spring with Linear Hysteresis

As shown in Figs. 2, 3 and 4, we assume that nonlinear concentrated springs with hysteresis have principal elastic axis in y direction. We denote displacement as $U_{my} (m = 1,2)$ in y -direction at the m -th nodal point where the nonlinear concentrated springs are connected with the T-shaped structure

having acoustic black hole in the one edge. Nonlinear function using power series is given for nodal force at the points m ($m = 1,2$). Therefore, the restoring force of the spring is expressed as $R_{my} = \gamma_{1my}U_{my} + \gamma_{3my}U_{my}^3$ when we consider cubic nonlinearity with the hardening characteristics as shown in Fig. 6. Further, linear hysteresis damping [11]-[13] is introduced as $\gamma_{1my} = \bar{\gamma}_{1my}(1 + \mathbf{j}\eta_s)$, $\bar{\gamma}_{1my}$ is the real part of γ_{1my} , and η_s is the material loss factor of the concentrated spring. \mathbf{j} is the imaginary unit. These relations can be rewritten in the matrix form as:

$$\{r_m\} = [\bar{\gamma}_{1m}]\{U_s\} + \{\bar{d}_m\} \quad (1)$$

$$\{r_m\} = \{r_{mx}, r_{my}, r_{mz}\}^T, r_{mx} = r_{mz} = 0, \{U_s\} = \{U_{mx}, U_{my}, U_{mz}\}^T, \{\bar{d}_m\} = \{0, \gamma_{3my}U_{my}^3, 0\}^T.$$

Where, $\{r_m\}$ is nodal force vector at the node m ($m = 1,2$). $\{U_s\}$ is the nodal displacement vector at the node m . $[\bar{\gamma}_{1m}]$ is the complex stiffness matrix involving only linear term of the restoring force. $\{\bar{d}_m\}$ is the vector containing nonlinear terms of the restoring force. In this paper, we set the restoring force with cubic nonlinearity as shown in Fig. 6.

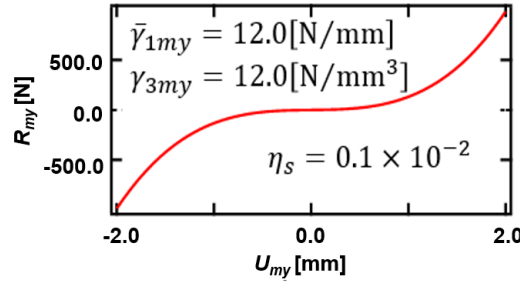


Fig. 6. Restoring force of nonlinear springs.

3.2 Discretized Equation of T-shaped Structure Having Acoustic Black Hole with Viscoelastic Layer

We assumed that equations of motion for the T-shaped structure having the acoustic black hole with the viscoelastic layer are expressed under infinitesimal deformation. Vibration damping of the metal structure having the acoustic black hole is taken into account using complex modulus of elasticity $E_{st} = \bar{E}_{st}(1 + \mathbf{j}\eta_{st})$. The real part \bar{E}_{st} of the E_{st} stands for the storage modulus of elasticity, while η_{st} is the material loss factor of the metal structure. In the same manner, vibration damping of the viscoelastic layer on the black hole is considered as $E_{vis} = \bar{E}_{vis}(1 + \mathbf{j}\eta_{vis})$. By superposing all elements related to the structure, the following equations in the entire domain of the T-shaped structure having acoustic black hole with the viscoelastic layer are obtained:

$$[M_p]\{\ddot{U}_p\} + [K_p]\{U_p\} = \{f_p\} \quad (2)$$

Where, $[M_p]$, $[K_p]$, $\{f_p\}$ and $\{U_p\}$ are the mass matrix, the complex stiffness matrix, the nodal force vector and the displacement vector, respectively. Isoparametric hexahedral elements with non-conforming modes [15] are mainly used for the numerical computation.

3.3 Discrete Equation for Combined System between T-shaped Structure Having Acoustic Black Hole and Nonlinear Concentrated Springs

The restoring force $\{r_m\}$ in Eq. (1) is added to the nodal force at the attached nodes m ($m = 1,2$) between the concentrated springs and the T-shaped structure. And then the following expression in global system can be obtained:

$$[M]\{\dot{U}\} + [K]\{U\} + \{\hat{d}\} = \{f\} \quad (3)$$

Where, $\{u\}, [M], [K], \{f\}$ are the displacement vector, the mass matrix, the complex stiffness matrix and the external force vector in global system, respectively. $\{\hat{d}\}$ is modified from $\{\bar{d}_m\}$ to have the identical vector size to degree- of- freedom of the Eq.(3).

3.4 Approximate Expression for Modal Damping [14]-[19]

By neglecting both the nonlinear term and the external force vector from Eq. (3), we can get the following complex eigenvalue problem:

$$\sum_{e=1}^{e_{\max}} \left([K_R]_e (1 + j\eta_e) - (\omega^{(i)})^2 (1 + j\eta_{\text{tot}}^{(i)}) [M]_e \right) \{\phi^{(i)*}\} = \{0\} \quad (4)$$

In this equation, superscript (i) stands for the i th eigenmode. $(\omega^{(i)})^2$ is the real part of complex eigenvalue. $\{\phi^{(i)*}\}$ is the complex eigenvector and $\eta_{\text{tot}}^{(i)}$ is the modal loss factor. $[K_R]_e$ is the real part of the element stiffness matrix.

Next, we introduce the following parameters β_e :

$$\beta_e = \frac{\eta_e}{\eta_{\max}}, \quad \beta_e \leq 1 \quad (5)$$

η_{\max} is the maximum value among the elements' material loss factors η_e , ($e = 1, 2, 3, \dots, e_{\max}$). On assumption of $\eta_{\max} \ll 1$, solutions of Eq. (4) are expanded using a small parameter $\mu = j\eta_{\max}$:

$$\{\phi^{(i)*}\} = \{\phi^{(i)}\}_0 + \mu\{\phi^{(i)}\}_1 + \mu^2\{\phi^{(i)}\}_2 + \dots \quad (6)$$

$$(\omega^{(i)})^2 = (\omega_0^{(i)})^2 + \mu^2(\omega_2^{(i)})^2 + \mu^4(\omega_4^{(i)})^2 + \dots \quad (7)$$

$$j\eta_{\text{tot}}^{(i)} = \mu\eta_1^{(i)} + \mu^3\eta_3^{(i)} + \mu^5\eta_5^{(i)} + \dots \quad (8)$$

In these equations, under conditions of $\beta_e \leq 1$ and $\eta_{\max} \ll 1$, we can obtain $\eta_{\max}\beta_e \ll 1$. Thus, $\mu\beta_e$ is regarded as small parameter like μ . In the equations, $\{\phi^{(i)}\}_0, \{\phi^{(i)}\}_1, \{\phi^{(i)}\}_2, \dots$ and $(\omega_0^{(i)})^2, (\omega_2^{(i)})^2, (\omega_4^{(i)})^2, \dots$ and $\eta_1^{(i)}, \eta_3^{(i)}, \eta_5^{(i)}, \dots$ have real quantities. Some parts of the mathematical procedures using Eqs. (5), (6), (7) and (8) are basically proposed by Ma [15] for linear problem having one viscoelastic material. We extended the procedures to general problem including multiple viscoelastic materials.

Substituting these equations from Eq. (6) to Eq. (8) into Eq. (4) yields the successive equations that the asymptotic solutions must satisfy:

μ^0 order:

$$\sum_{e=1}^{e_{\max}} \left([K_R]_e - (\omega_0^{(i)})^2 [M]_e \right) \{\phi^{(i)}\}_0 = \{0\} \quad (9)$$

μ^1 order:

$$\sum_{e=1}^{e_{max}} \left(\mu \beta_e [K_R]_e - \mu \eta_1^{(i)} (\omega_0^{(i)})^2 [M]_e \right) \{\phi^{(i)}\}_0 + \sum_{e=1}^{e_{max}} \left(\mu [K_R]_e - \mu (\omega_0^{(i)})^2 [M]_e \right) \{\phi^{(i)}\}_1 = \{0\} \quad (10)$$

Furthermore, by arranging Eq. (9) and Eq. (10), the following equation can be derived:

$$\eta_{tot}^{(i)} = \sum_{e=1}^{e_{max}} (\eta_e S_e^{(i)}), \quad S_e^{(i)} = \frac{\{\phi^{(i)}\}_0^T [K_R]_e \{\phi^{(i)}\}_0}{\sum_{e=1}^{e_{max}} \{\phi^{(i)}\}_0^T [K_R]_e \{\phi^{(i)}\}_0} \quad (11)$$

According to these expressions, modal loss factor $\eta_{tot}^{(i)}$ can be calculated using material loss factors η_e of each element e and share $S_e^{(i)}$ of strain energy of each element to total strain energy. The eigenmodes $\{\phi^{(i)}\}_0$ in Eq. (11) are real. Therefore, the eigenmodes can be easily obtained by solving familiar real eigenvalue problem Eq. (9), which corresponds to the equation by deleting all damping term in Eq. (4). Equation (11) has identical formation to Modal Strain Energy Method [14]-[19], resultantly.

3.5 Conversion from the Discretized Equation in Physical Coordinate to the Nonlinear Equation in Normal Coordinate

It takes large amount of computational time to calculate Eq. (3) in physical coordinate, directly. In this section, a numerical manipulation is carried out to decrease the degree-of-freedom for the discretized equations of motion [11]-[13].

First, we assume that linear natural modes $\{\phi^{(i)}\}$ of vibration can be approximated to $\{\phi^{(i)}\}_0$. Next, by introducing normal coordinates \tilde{b}_i corresponding to the linear natural modes $\{\phi^{(i)}\}_0$, the nodal displacement vector $\{U\}$ can be expressed using both $\{\phi^{(i)}\}_0$ and \tilde{b}_i as follows.

$$\{U\} = \sum_i \tilde{b}_i \{\phi^{(i)}\}_0 \quad (12)$$

Substitution of Eq. (12) into Eq. (3) yields the following nonlinear ordinary simultaneous equations as to normal coordinates \tilde{b}_i as:

$$\ddot{\tilde{b}}_i + \eta_{tot}^{(i)} \omega^{(i)} \dot{\tilde{b}}_i + (\omega^{(i)})^2 \tilde{b}_i + \sum_j \sum_k \sum_l \tilde{E}_{ijkl} \tilde{b}_j \tilde{b}_k \tilde{b}_l - \tilde{P}_i = 0 \quad (13)$$

$$\tilde{E}_{ijkl} = \sum_{m=1}^2 \gamma_{3my} \tilde{\phi}_{imy} \tilde{\phi}_{jmy} \tilde{\phi}_{lmy}, \quad \tilde{P}_i = \{\phi^{(i)}\}_0^T \{f\} \quad (14)$$

$(i, j, k, l = 1, 2, 3, \dots)$

Since Eq. (13) has much smaller degree-of-freedom than that of Eq. (3), computational time become less. ϕ_{imy} is the y-component of the eigenmode $\{\phi^{(i)}\}_0$ at the connected node m between the T-shaped structure having the acoustic black hole and the nonlinear concentrated spring. In this analysis, $\eta_{tot}^{(i)}$ is derived using the shares of strain energy on condition of linear small amplitude as described in Section 3.4.

By applying Runge-Kutta-Gill to Eq. (13), nonlinear impulse responses were calculated. In this numerical integration, an impulse was given for the force vector $\{f\}$ in Eq. (13) at the node β , which corresponds to the excitation point.

4. Results and Discussion

4.1 Validity of Computation Method for a Flat Plate Having Krylov's Acoustic Black Hole.

We reported [20] that damped vibration responses for a flat plate with the Krylov type acoustic black hole using our codes and our MSKE method with 3D FEM. In that report, we compared between Krylov's experiment [5] and our numerical results to check the validity. In the edge of the panel with the black hole, the function of decreasing thickness $h(x)$ was $h(x)=\epsilon x^m$ ($m=2.2$), where x was distance from the edge. This function was same with that of the T-shaped structure in this paper. From these results, our computation could reproduce the black hole effects in the past experiment.

4.2 Modal Loss Factors from Eigen Value Analysis with MSE Method

Figure 7 represents comparison of modal loss factors with /without the acoustic black hole and the residual thickness and the viscoelastic layer. The ordinate is the modal loss factor, while the abscissa is the mode ID having similar deformations among three models for the T-shaped structures. As can be seen in this figure, by adding the acoustic black hole to the T-shaped structures, modal loss factors significantly increase. Further, modal loss factors of some modes become higher due to set the residual thickness.

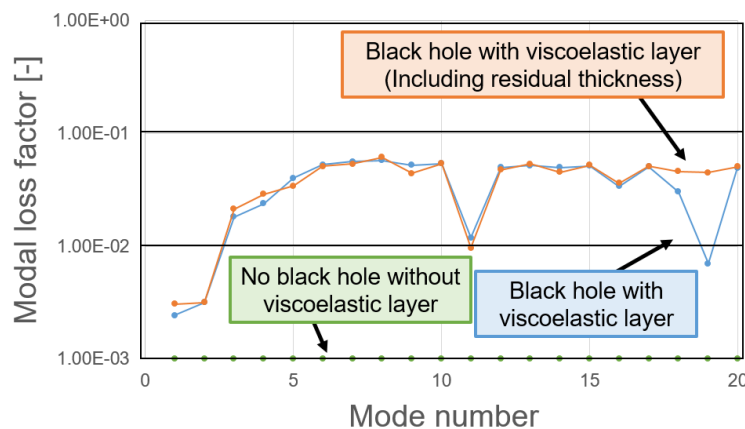


Fig. 7. Comparison of modal loss factors with /without acoustic black hole and residual thickness and viscoelastic layer.

4.3 Results of Impact Responses

To investigate influences of nonlinear coupling in vibration among the T-shaped structures having the acoustic black holes and the nonlinear springs, we studied nonlinear vibration phenomena under impact force. Figure 8 represents an evaluation flow of impact responses.

An impact pulse in the y -direction shown in Fig. 8 is given for the force vector $\{f\}$ of \tilde{P}_i in Eq. (13) at the node β , which is excitation point as we specified in Fig. 5. Time histories of the nonlinear impact responses are calculated by applying Runge-Kutta-Gill method to Eq. (13). We compute nonlinear transient time histories by varying the maximum amplitude $|f_{\max}|$ of the impact under a constant pulse width 0.001 [s]. And we calculate displacement w at the evaluation point shown in Fig. 5. Figures 9, 10 and 11 show the frequency response functions of the time histories under the small impact force $|f_{\max}| = 9.8[\text{N}]$. In Figs. 9, 10 and 11, the abscissa shows Fourier frequency ω_{sp} , while the ordinate represents amplitude of frequency response function $A(\omega_{\text{sp}})$. For $A(\omega_{\text{sp}})$, 0 [dB] represents that the amplitude of the spectrum equals 1 mm.

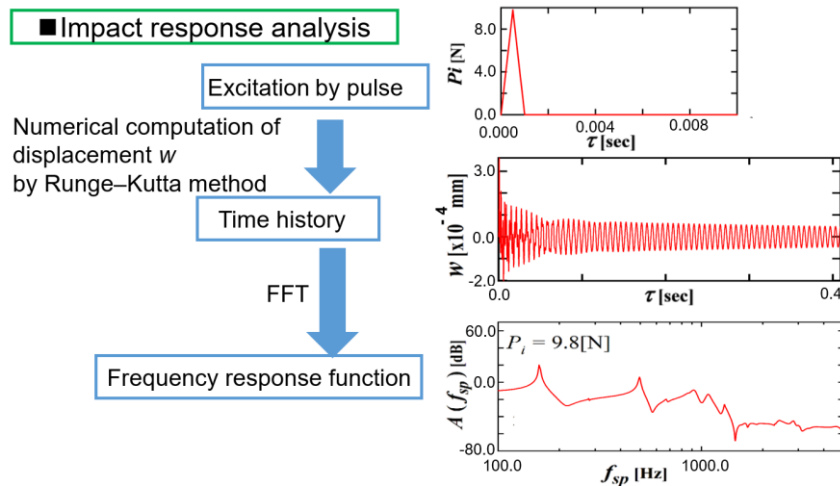


Fig. 8. Evaluation flow of impact responses for T-shaped structures.

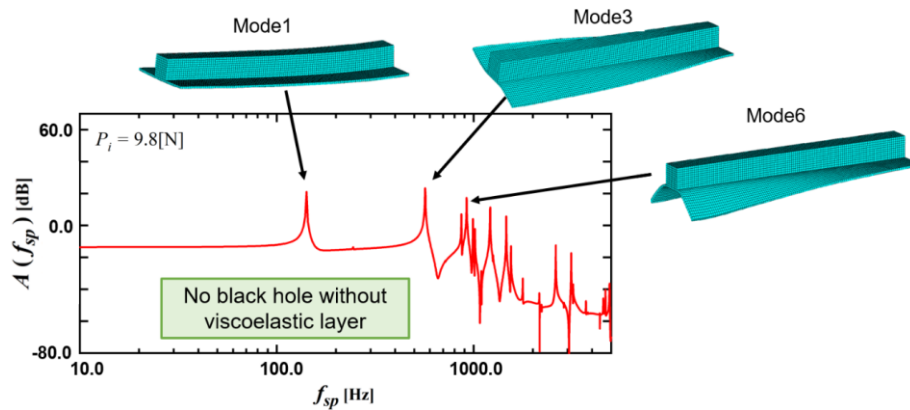


Fig. 9. Impact response for T-shaped structure with no acoustic black hole and viscoelastic layer under small force amplitude.

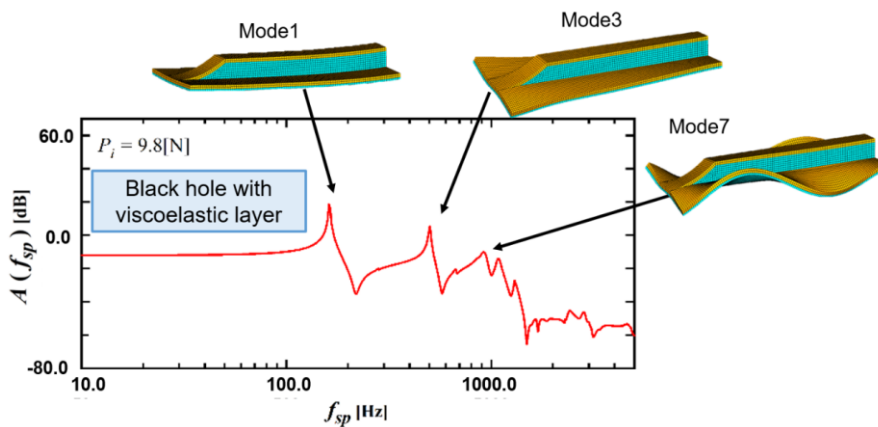


Fig. 10. Impact response for T-shaped structure with acoustic black hole and viscoelastic layer under small force amplitude.

Under the small input force $|f_{\max}| = 9.8 \text{ N}$ in Figs. 9, 10 and 11, some eigenmodes corresponding to the typical peaks in the frequency response functions are written. These modes include the large deformations in the nonlinear springs. In Fig. 9, the peaks of the modes 1, 3 and 6 appear. In Fig. 10, the peaks of the modes 1, 3 and 7 appear. In Fig. 11, the peaks of the modes 1, 3 and 5 appear. However, we cannot find out nonlinear responses in Figs. 9, 10 and 11 because of the small impact force.

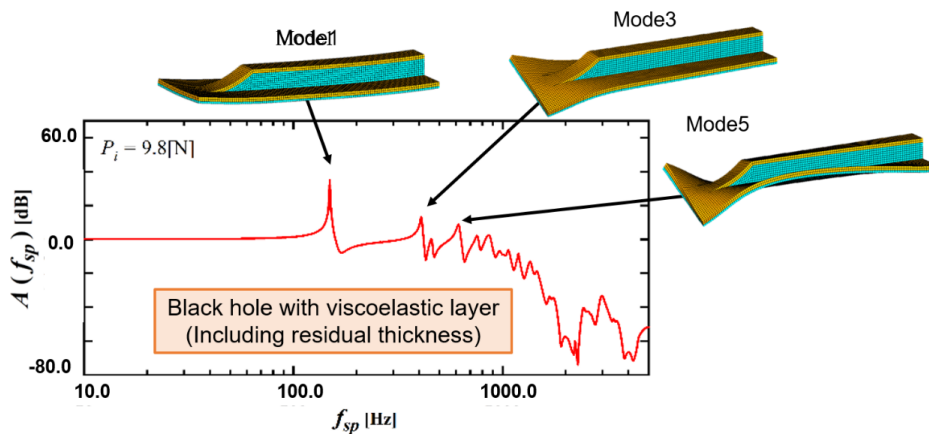


Fig. 11. Impact response for T-shaped structure with acoustic black hole and viscoelastic layer including residual thickness under small force amplitude.

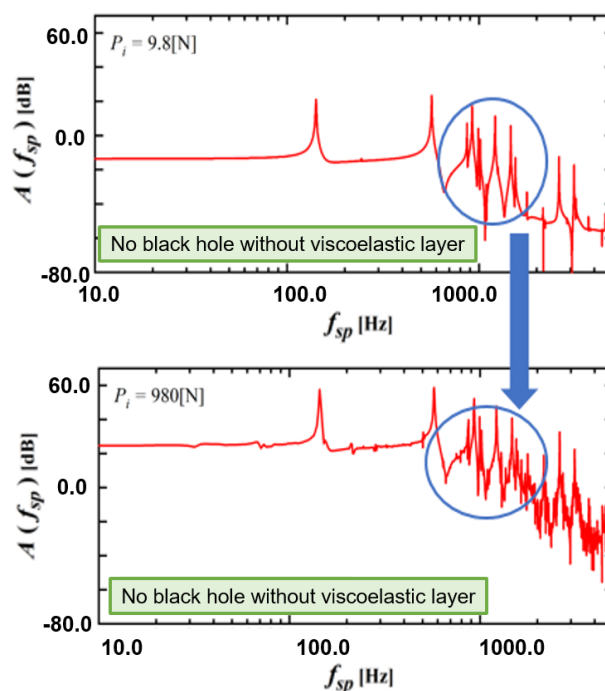


Fig. 12. Influences of force amplitudes on impact response for T-shaped structure with no acoustic black hole and no viscoelastic layer.

For the case without the black hole and without the viscoelastic layer in Fig. 9, all resonances have sharp peaks because of low damping. For the case with the black hole and with the viscoelastic layer in Fig. 10, amplitudes of resonance peaks decrease in comparison with those in Fig. 9 due to high damping. Especially, amplitudes of the peaks in the higher frequency decrease much more because the damping effects of the black hole increase. For the case with the black hole including the residual thickness and with the viscoelastic layer in Fig. 11, amplitudes of the peaks reduce more than those in Fig. 10. This phenomenon is caused by adding the residual thickness.

As excitation force increases for the T-shaped structure with no acoustic black hole and no viscoelastic layer, new peaks are appeared as shown in Fig. 12. We can observe the generation of the super-harmonic components and the sub-harmonic components of the peaks corresponding to the modes having large deformations in the nonlinear springs.

Figure 13 corresponds to the frequency response functions of the time histories under the large impact force $|f_{\max}| = 980$ N for the T-shaped structures with / without the acoustic black hole and

viscoelastic layer and residual thickness. As we can see, the nonlinear components decrease when the acoustic black holes are added to the T-shaped structure. Further, if the residual thickness is set to the acoustic black hole, the nonlinear components are much more reduced.

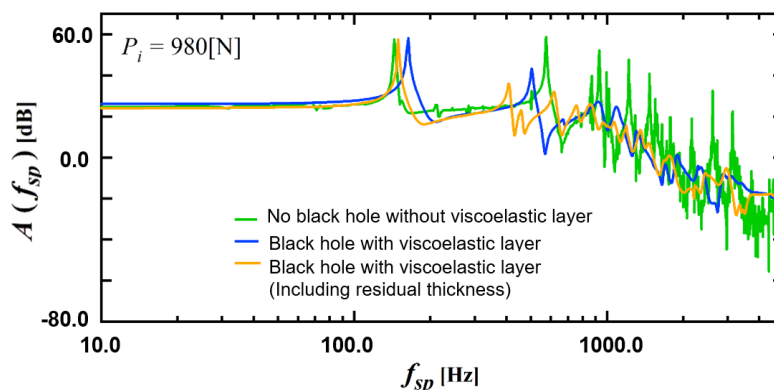


Fig. 13. Nonlinear impact responses for T-shaped structures with/without acoustic black hole and viscoelastic layer and residual thickness under large force amplitude.

We will continue to study the basic characteristics of these new structures using our proposed acoustic black hole. After more investigations under many conditions, we will clarify merits and practical limitations.

5. Conclusions

To clarify nonlinear vibration characteristics of T-shaped structures having acoustic black holes with viscoelastic damping layers supported by nonlinear springs, we compute nonlinear transient responses. We added acoustic black hole at one edge of the T-shaped structure. We give the new acoustic black holes at one edge of the rib in the T-shaped structures. Around the edge of the rib plate, the height of the rib decreases according to the function for the Krylov's acoustic black hole. We clarified influences of amplitude of the impact force on nonlinear transient responses for the structure. Effectiveness of acoustic black holes are investigated to decrease nonlinear vibration under large force amplitudes. By adding the acoustic black hole to the T-shaped structures, modal loss factors increase. Higher modal loss factors are obtained due to set the residual thickness. As the amplitude of the impact force increase on the T-shaped structure with no acoustic black hole and viscoelastic damping layer, the responses become complicated due to the nonlinearity, and include more super harmonic and subharmonic components. These nonlinear components are reduced by adding the acoustic black hole. The much less nonlinear components are given due to set the residual thickness.

Acknowledgement

This research is supported by Suzuki Foundation Research Grant.

References

- [1] M.A. Mironov, "Propagation of a flexural wave in a plate whose thickness decreases smoothly to zero in a finite interval", *Soviet Physics-Acoustics*, Vol.34, pp.318–319, 1988.
- [2] V.V. Krylov, "Laminated plates of variable thickness as effective absorbers for flexural vibrations", *Proceedings of the 17th ICA* (Rome, Italy), September 2001.
- [3] V.V. Krylov, F.J.B.S. Tilman, "Acoustic 'black holes' for flexural waves as effective vibration dampers", *Journal of Sound and Vibration*, Vol.274(3–5), pp.605–619,2004.
- [4] V.V. Krylov, "New type of vibration dampers utilizing the effect of acoustic 'black holes' ", *Acta Acustica united with Acustica*, Vol.90(5), pp.830–837, 2004.

- [5] V.V. Krylov, V. Kralovic, D.J. O'Boy, "Damping of flexural vibrations in rectangular plates using the acoustic black hole effect", *Journal of Sound and Vibration*, Vol.329, pp.4672-4688,2010.
- [6] H.Oberst, *Akustische Beihefte* , Vol.4, pp.181-194,1952.
- [7] L. Tang, L. Cheng and H. Ji, J. Qiu, "Enhanced acoustic black hole effect using a modified thickness profile", *Proceedings of INTER NOISE CONFERENCE 2016*, (Hamburg, Germany), pp.2361-2369, , July 2016.
- [8] T. Koizumi, T. Yamaguchi, S. Maruyama, K. Takebayashi and M. Tsushima, "Impact response analysis of a structure supported by non-linear springs on steel plate with an acoustic black hole", *Proceedings of the 31th JSME Computational Mechanics Conference* (Tokushima, Japan), 18-8-113, pp.1-4, September 2018.
- [9] B. F. Feeny and R. Kappagantu, "On the physical interpretation of proper orthogonal modes in vibrations", *Journal of Sound and Vibration*, Vol.211(4), pp. 607-616, 1998.
- [10] E. Pesheck, N. Boivin, C. Pierre and S. W. Shaw, "Nonlinear modal analysis of structural systems using multi-mode invariant manifolds", *Nonlinear Dynamics*, Vol. 2, pp. 183-205, 2001.
- [11] T. Yamaguchi, Y. Fujii, K. Nagai and S. Maruyama, "FEM for vibrated structures with non-linear concentrated spring having hysteresis", *Mechanical Systems and Signal Processing*, Vol.20, pp. 1905-1922, 2006.
- [12] T. Yamaguchi, T. Saito, K. Nagai, S. Maruyama, Y. Kurosawa and S. Matsumura, "Analysis of damped vibration for a viscoelastic block supported by a nonlinear concentrated spring using FEM", *Journal of Environment and Engineering*, Vol. 2 (3), pp. 578-589, 2007.
- [13] T. Yamaguchi, H. Hozumi, Y. Hirano, K. Tobita, and Y. Kurosawa, "Nonlinear transient response analysis for double walls with a porous material supported by nonlinear springs using FEM and MSKE method", *Mechanical Systems and Signal Processing*, Vol.42, pp.115-128, 2014.
- [14] C. D. Johnson and D. A. Kienholz, "Finite element prediction of damping structures with constrained viscoelastic layers", *AIAA Journal*, Vol.20(9), pp.1284-1290, 1982.
- [15] B. A. Ma, and J. F. He, "A finite element analysis of viscoelastically damped sandwich plates", *Journal of Sound and Vibration*, Vol.152(1), pp.107-123, 1992.
- [16] T. Yamaguchi, Y. Kurosawa and S. Matsumura, "FEA for damping of structures having elastic bodies, viscoelastic bodies, porous media and gas", *Mechanical Systems and Signal Processing*, Vol.21(1), pp.535-552, 2007.
- [17] T. Yamaguchi, I. Shirota, H. Enomoto and Y. Kurosawa, "Vibration transmission between double walls in cars with damping and sound bridges", *Noise Control Engineering Journal*, Vol.58(3), pp.273-282, 2010.
- [18] T. Yamaguchi, Y. Kurosawa and H. Enomoto, "Damped vibration analysis using finite element method with approximated modal damping for automotive double walls with a porous material", *Journal of Sound and Vibration*, Vol.325, pp.436-450, 2009.
- [19] K. Takebayashi, A. Tanaka, K. Andow and T. Yamaguchi, "Modal loss factor approximation for u-p formulation FEM using modal strain and kinetic energy method", *Journal of Sound and Vibration*, Vol.505, pp.1-14, 2021.
- [20] T. Tsuboi, T. Yamaguchi, S. Maruyama, T. Okada and K. Takebayashi, "SEA response analysis using FEM for two panels connected in L-shape having an acoustic black hole and damping layers", *Proceedings of the 30th JSME Computational Mechanics Conference* (Osaka, Japan), 17-4, 133, pp.1-3, September 2017.